European Polymer Journal 46 (2010) 1397–1403

Contents lists available at ScienceDirect

European Polymer Journal

journal homepage: www.elsevier.com/locate/europolj

Macromolecular Nanotechnology

Nanostructured thermoresponsive quantum dot/PNIPAM assemblies

Oya Tagit [a,b], Dominik Jańczewski [c], Nikodem Tomczak [c], Ming Yong Han [c,d], Jennifer L. Herek [b], G. Julius Vancso [a,*]

[a] Materials Science and Technology of Polymers, Faculty of Science and Technology and MESA+ Institute for Nanotechnology, University of Twente, P.O. Box 217, 7500 AE Enschede, The Netherlands

[b] Optical Sciences, Faculty of Science and Technology and MESA+ Institute for Nanotechnology, University of Twente, P.O. Box 217, 7500 AE Enschede, The Netherlands

[c] Institute of Materials Research and Engineering, A*STAR (Agency for Science, Technology and Research), 3 Research Link, Singapore 117602, Singapore

[d] Division of Bioengineering, Faculty of Engineering, National University of Singapore, Singapore 117576, Singapore

ARTICLE INFO

Article history:
Received 8 April 2010
Received in revised form 23 April 2010
Accepted 27 April 2010
Available online 5 May 2010

Keywords:
Stimuli responsive polymer
PNIPAM
Quantum dots
Reversible switching of luminescence

ABSTRACT

Synthesis, characterization, and applications of novel thermoresponsive polymeric coatings for quantum dots (QDs) are presented. Comb-copolymers featuring hydrophobic alkyl groups, carboxylic groups and poly(*N*-isopropylacrylamide) (PNIPAM) side chains with molar masses ranging from 1000 g/mol to 25,400 g/mol were obtained. The amphiphilic comb-copolymers were shown to efficiently transfer the QDs to aqueous media. The PNIPAM-coated QD materials display a lower critical solution temperature (LCST). The absorbance, luminescence emission, size of the assemblies, and electrophoretic mobility were followed as a function of temperature and the reversibility of the temperature induced changes is demonstrated by cyclic heating and cooling.

1. Introduction

Stimulus responsive organic–inorganic hybrid materials find applications in drug delivery [1], bionanotechnology [2,3], and sensing [4] among other areas. The organic part of the hybrids is made of so-called "smart" polymers, i.e., polymers that undergo conformational changes in response to external stimuli such as temperature [5], pH [6], or solvent [7]. Poly(*N*-isopropyl acrylamide), PNIPAM, is probably the best-known and the most-studied thermoresponsive polymer exhibiting a lower critical solution temperature (LCST). Below the critical transition, the polymer is hydrophilic and disperses well in aqueous solutions. Above the LCST (~32 °C for PNIPAM), the polymer becomes hydrophobic. Thus, at or above the LCST the polymer deswells and the chains collapse [8]. The LCST behavior of PNIPAM has been widely explored for drug delivery [9] and sensing applications [10]. The inorganic part of the hybrids may serve not only as a scaffold for the organic part but may also display functionalities such as magnetic or luminescent properties. Regarding hybrid materials, thermoresponsive polymeric coatings have been applied to magnetic iron oxide [1,3,4,11–14], gold [15–22], and silica nanoparticles [18,23–25].

Semiconductor nanoparticles such as quantum dots (QDs) gained much attention as luminescent materials due to their unique composition and size-tunable properties, broad excitation and narrow emission spectra, and high photochemical stability [26]. Combining QDs with thermoresponsive coatings, such as PNIPAM, has not yet been widely explored [27]. Hybrid thermoresponsive polymer/QD assemblies have previously been prepared by grafting end-functionalized polymer chains [28,29], surface initiated polymerization [30], hydrogen bond formation [31], or solvent induced encapsulation [32]. Alternatively, one can employ amphiphilic polymers to coat the surface of hydrophobic QDs [33–35]. A major advantage of amphiphilic coatings is the ability to introduce diverse functionalities at the QD surface. Coatings

* Corresponding author. Address: Materials Science and Technology of Polymers, Faculty of Science and Technology, and MESA+ Institute for Nanotechnology, University of Twente, P.O. Box 217, 7500 AE Enschede, The Netherlands. Tel.: +31 53 4892971; fax: +31 53 4893823.
E-mail address: g.j.vancso@tnw.utwente.nl (G.J. Vancso).

0014-3057/$ - see front matter © 2010 Elsevier Ltd. All rights reserved.
doi:10.1016/j.eurpolymj.2010.04.026

with grafted polymer side chains can also be prepared, and a one-step coating procedure may be employed to prepare QDs with grafted polymer chains. Such a coating would endow the QDs with water-dispersability and thermoresponsiveness. Application of amphiphilic coatings with thermoresponsive side polymer chains for QDs, however, has not been studied to date. The limitations imposed on the molar mass of the polymer side chains for effective transfer of the QDs to water using amphiphilic polymers are also not known. The molar mass of the thermoresponsive polymer grafted onto the nanoparticles may in addition influence the thermally induced collapse of the hybrids [20]. Thus, consideration should be given to the molar mass of the thermoresponsive polymeric coatings on the QD surface, as well.

In this study, we show that aqueous dispersions of hybrid PNIPAM/QD assemblies can be prepared using TOPO-coated QDs and engineered polymeric coatings. The coatings consist of an amphiphilic polymer bearing PNIPAM side chains. CdSe/ZnS QDs are grafted with PNIPAM chains with molar masses of 1.0×10^3, 10.8×10^3, and 25.4×10^3 g/mol and are transferred into water. The hybrid materials exhibit a well-pronounced LCST behavior. Above the LCST the PNIPAM chains on the surface of the QDs become hydrophobic and collapse. However, the presence of carboxylate groups on the amphiphilic coating prevents the nanoparticles from aggregating. As a result, higher electrophoretic mobility is observed above LCST. The transition is fully reversible, as observed during a number of heating and cooling cycles.

2. Experimental

2.1. Materials

Core–shell CdSe/ZnS QDs were synthesized in the presence of trioctylphosphine oxide (TOPO), triphenylphosphine (TOP) and *n*-hexadecylamine according to the reported procedure [35]. The size of the QDs was controlled by the reaction temperature and the time elapsed until the shell material was added to the reaction mixture after the initial core formation. Reaction at 235 °C for 30 min resulted in red-emitting QDs with a first absorption peak located at 620 nm and with a narrow emission spectrum (35 nm full width at half maximum) with a peak located at 638 nm. The quantum yield of the QDs was calculated using a tris-(2,2′-bipyridine)ruthenium (II) (Ruthenium–BPY complex) as the reference. Amino-terminated PNIPAM (NH_2-PNIPAM) with three different molar masses (M_w) 1.0×10^3, 10.8×10^3, and 25.4×10^3 g/mol were purchased from Polymer Source Inc. (Canada). *n*-Octylamine, *N*,*N*-diisopropylethylamine (DIPEA), poly(isobutylene-alt-maleic anhydride) (M_w = 6000 g/mol, M_w/M_n = 1.7), and other chemicals were purchased from Sigma–Aldrich.

2.2. Synthesis of polymer 1 (***P1***)

n-Octylamine (0.4 mL) and 1.0 mL of DIPEA, were added to 300 mL of a THF solution containing 0.35 g of poly (isobutylene-alt-maleic anhydride) and stirred until a clear solution was obtained. One gram of PNIPAM (1×10^3 g/mol, M_w/M_n = 1.8) was added to the solution and the reaction was left to proceed for 12 h at 50 °C. Subsequently THF was evaporated and the resulting material was suspended in water with small excess of NaOH (pH 11) with respect to the carboxylic groups on the polymer backbone. After evaporation of water and DIPEA, the remaining residue was dissolved in water and dialyzed using a cellulose membrane against 0.01 M NaOH and pure water for a week. Evaporation of water by freeze-drying resulted with 0.4877 g of polymer **P1** as white powder. The polymer composition was determined by ^{1}H NMR: δ_H(400 MHz; D_2O): 7.35 (9 H, br), 3.93 (153 H, br), 3.77–2.45 (112 H, m), 2.45–1.85 (255 H, m), 1.85–1.47 (350 H, br), 1.38 (253 H, br), 1.20 (921 H, br), 1.15–0.82 (284 H, m) (see Supporting information).

2.3. Synthesis of polymer 2 (***P10***)

n-Octylamine (0.06 mL) and 0.15 mL of DIPEA, were added to 300 mL of a THF solution containing 0.14 g of poly (isobutylene-alt-maleic anhydride) and stirred until a clear solution was obtained. One gram of PNIPAM (10.8×10^3 g/mol, M_w/M_n = 1.55) was added to the solution and the same procedure used for the synthesis of **P1** was applied. The polymer composition was determined by ^{1}H NMR: δ_H(400 MHz; D_2O): 7.34 (7 H, br), 3.93 (281 H, br), 3.79–2.45 (102 H, m), 2.45–1.88 (362 H, m), 1.85–1.42 (539 H, br), 1.33 (257 H, br), 1.18 (1687 H, br), 1.15–0.82 (285 H, m).

2.4. Synthesis of polymer 3 (***P25***)

n-Octylamine (0.12 mL) and 0.3 mL of DIPEA, were added to 300 mL of a THF solution containing 0.31 g of poly (isobutylene-alt-maleic anhydride) and stirred until a clear solution was obtained. One gram of PNIPAM (25.4×10^3 g/mol, M_w/M_n = 2.49) was added to the solution and the same procedure used for the synthesis of **P1** was applied. The polymer composition was determined by ^{1}H NMR: δ_H(400 MHz; D_2O): 7.33 (9 H, br), 3.92 (92 H, br), 3.79–2.45 (68 H, m), 2.45–1.84 (167 H, m), 1.84–1.42 (213 H, br), 1.32 (179 H, br), 1.17 (567 H, br), 1.15–0.75 (266 H, m).

2.5. Coating of QDs with amphiphilic polymers

Three milligrams of purified QDs were suspended in 3 mL of THF. About 30, 60, and 30 mg, of polymers **P1**, **P10**, and **P25**, respectively, were dissolved in 2 mL of water. The polymer and QD solutions were mixed while purging with argon. Following the evaporation of THF and half of the volume of water, the solutions were diluted with 2 mL of water. The resulting aqueous solutions of polymer-coated QDs **R1**, **R10**, and **R25** were filtered through a 0.22 μm MILEX PES membrane filter and centrifuged at 10,000 rpm for 30 min. These solutions were directly used for the absorption and emission measurements.

2.6. Characterization methods

^{1}H NMR spectra were obtained using a Bruker spectrometer (DRX 400 MHz). UV–vis absorption was recorded using a Shimadzu spectrophotometer (UV-1601). A Cary Eclipse spectrofluorometer with a Peltier thermoelectric cuvette holder was used to obtain the luminescence spectra of the QD solutions. Particle size and surface charge measurements were performed with a Zetasizer Nano ZS (Malvern Instruments, Malvern, UK) equipped with a He–Ne laser (633 nm, 4 mW). The scattered light was collected at 173°.

3. Results and discussion

The absorption and emission spectra of the TOPO-coated CdSe/ZnS core/shell QDs are shown in Fig. 1. The core size of the QDs was estimated to be equal to ~5.6 nm by using the reported empirical equation [36].

Our strategy to fabricate QD materials with temperature responsiveness is based on the design of suitable polymeric coatings for QDs, which include functional parts composed of PNIPAM. To this end, we have employed an amphiphilic polymer structure, which was already reported to efficiently coat hydrophobically-functionalized QDs [35]. A number of different functionalities including bulky side groups and longer PEG chains appended to the amphiphilic polymer were shown not to preclude the transfer of the QDs into water. The synthesis of functionalized amphiphilic polymers is based on anhydride ring opening with amine-functionalized molecules in presence of an amine catalyst. For the polymer to serve as an efficient amphiphilic coating one needs to include hydrophobic side groups for interactions with the hydrophobic ligands on the QD surface, and hydrophilic groups to attain colloidally stable suspension of the nanoparticles in water. Reaction of the anhydride polymer backbones with *n*-octylamine and amine-terminated PNIPAM of different molar masses resulted in a series of amphiphilic polymers with a general structure shown in Fig. 2.

Upon completion of the reaction the amphiphilic polymers include octyl side groups for interaction with TOPO present on the QD surface, carboxyl groups for water-dispersability and PNIPAM chains to induce temperature responsiveness. The compositions of polymers **P1**, **P10**, and **P25** were evaluated by ^{1}H NMR and are presented in Table 1.

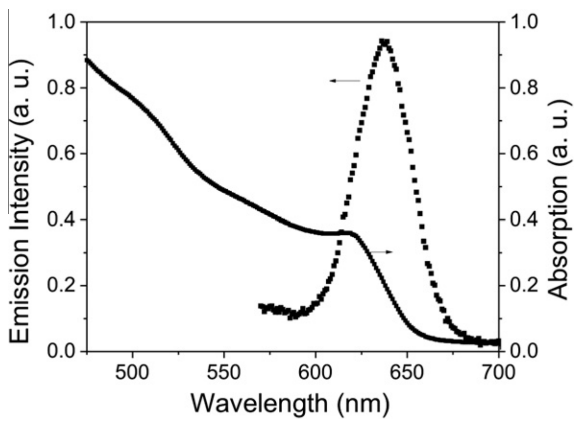

Fig. 1. Normalized absorption and emission spectra of TOPO-coated CdSe/ZnS QDs in chloroform solution.

The number of PNIPAM chains *per* poly(isobutylene-*alt*-maleic anhydride) backbone was equal to 19, 3, and 0.4 for polymers **P1**, **P10**, and **P25**, respectively. All polymers displayed an LCST with a transition onset occurring at temperatures to within 1 °C equal to that of the PNIPAM (Fig. 3). Therefore, grafting of the PNIPAM chains to the anhydride backbone did not modify their LCST behavior.

Hydrophobic TOPO-coated QDs were transferred from organic solution to water using polymers **P1**, **P10**, and **P25**; as a result assemblies **R1**, **R10**, and **R25** were formed. All polymers efficiently coated the QD surface rendering the QD/polymer assemblies hydrophilic.

The absorption and emission spectra of QDs **R1**, **R10**, and **R25** coated with the polymers **P1**, **P10**, and **P25**, respectively, are shown in Fig. 4. The position of the first absorption peak and that of the emission peak was not altered significantly by the presence of the polymeric coating. However, the emission intensity clearly decreased in comparison with TOPO-coated QDs of the same concentration (data not shown). The quantum yields of the samples were determined using a Ruthenium–BPY complex as reference and were found to be equal to 60% (unmodified QDs), 37% (**R1**), 14% (**R10**), and 35% (**R25**). Although such a decrease in QYs was reported previously for hydrophilic, polymer-coated QDs [34], we cannot rule out that other factors, including multiple particle aggregation play here a role. Once transferred to water the PNIPAM-coated QDs displayed colloidal stability for a period of several months with no visible precipitation. The stability of the polymer coating covering the QD surface is a result of hydrophobic–hydrophobic interactions between the octylamine groups of the polymer with the TOPO layer at the QD surface. The colloidal stability of QD/PNIPAM assemblies in water is provided by the hydrophilic nature of PNIPAM and the carboxyl groups on the polymer backbone.

In order to characterize the temperature response of QDs coated with the new amphiphilic coatings, a series of temperature-dependent absorption and emission measurements was performed (Fig. 5). Upon reaching temperatures above the LCST, the absorbance of samples **R1**, **R10**, and **R25** increased. A sharp transition at 32 °C was observed for sample **R25**. The transitions for samples **R10** and **R1** occurred at 34 and 33 °C, respectively.

Interestingly, the QD luminescence emission intensity was also influenced by temperature. Pronounced transitions in the luminescence intensity for all polymer-coated QD samples, as shown in Fig. 5, occurred to within the experimental error at the same temperatures as the transitions visible in the absorbance. This suggests that the LCST behavior of PNIPAM was responsible for the changes in the luminescence emission of the QDs. We performed a control experiment, where we heated the same QDs coated with a PEG-modified amphiphilic polymer [35] instead of PNIPAM. No transition was observed within the probed temperature range, and the changes in the emission intensity followed a similar trend as reported in the literature [5]. This indicates that changes within the PNIPAM shell were responsible for the observed behavior.

The transitions in absorption and luminescence associated with the LCST of PNIPAM were clearly reversible (Fig. 5). The absorption and the luminescence intensities

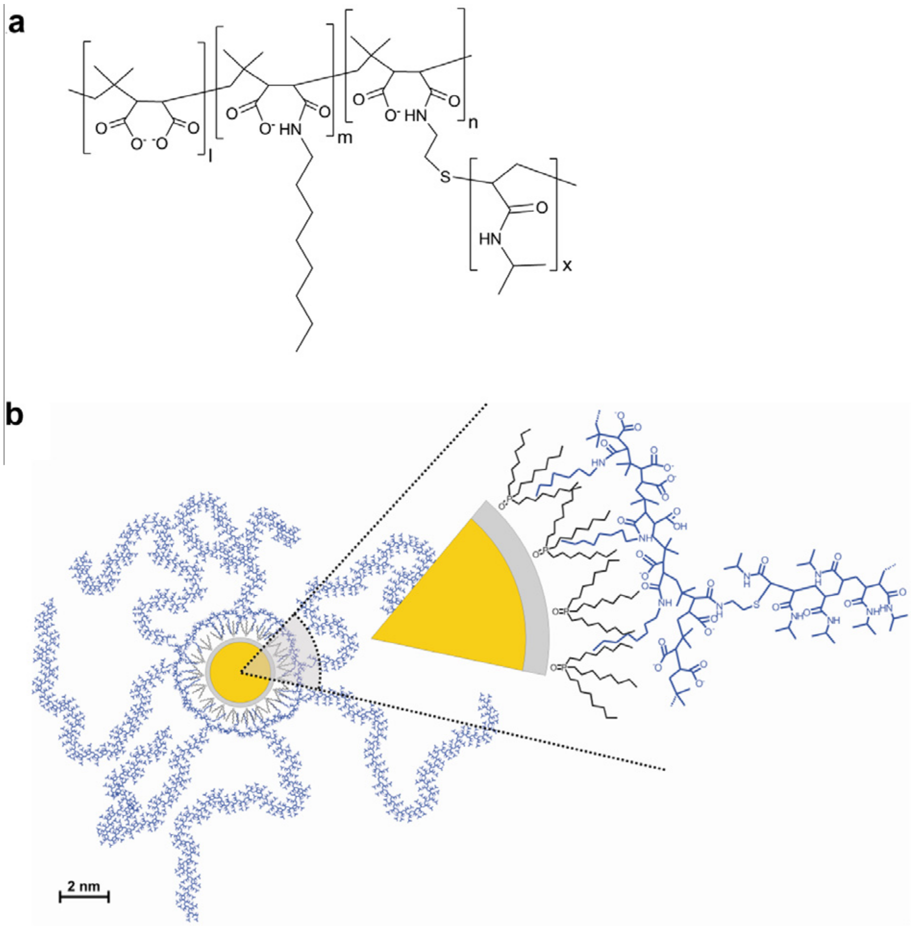

Fig. 2. (a) Schematic structure of the amphiphilic polymeric coatings after grafting of NH_2-terminated PNIPAM and *n*-octylamine. ($l + m + n = 38$) to a poly(isobutylene-*alt*-maleic anhydride) backbone. The number of monomer units in the PNIPAM chain is denoted with *x*. (b) Schematic representation of a TOPO-QD coated with the amphiphilic polymeric coating bearing PNIPAM side chains. The zoomed-in section shows details of the polymeric coating.

Table 1
Composition of amphiphilic, PNIPAM-functionalized polymers used to transfer QDs into water.

Polymer	$M \times 10^{3a}$ [g/mol]	PNIPAM $M \times 10^3$ (g/mol)	Indices *l*, *m*, *n*, *x*	% of functional groups		
				Carboxylic	*n*-Octyl amide	PNIPAM
P1	28.7	1	0, 19, 19, 8	50	25	25
P10	41.9	10.8	16, 19, 3, 95	71	25	4
P25	19.8[b]	25.4	25, 13, 0.4, 220	82.7	16.7	0.6

[a] Number average molar mass calculated from the NMR spectra.
[b] Average molar mass for a mixture of two polymers [considering the size of PNIPAM side chain and the fact that $n = 0.4$ there are most likely two types of chains present, one without any PNIPAM side chain ($n = 0$ $M_w = 9000$ g/mol) and with a single PNIPAM side chain ($n = 1$, $M_w = 34\,000$ g/mol)].

recovered back to the initial values when the temperature was decreased below the LCST. Similar trends in the emission and absorption, including the extent of the hysteretic behavior was observed for each of the samples, giving additional evidence that PNIPAM is responsible for the observed changes. The reversibility of the LCST-induced transitions was also studied by heating above LCST to 50 °C and cooling down to 25 °C over multiple heating/cooling cycles (Fig. 6). To compare the influence of temperature on the absorption and emission intensities for different samples, the initial values were normalized to 0.1 for absorption and to 1.0 for emission.

Different response to changes in temperature depending on the polymer coating is a result of a convolution of different factors including the molar mass of the grafted PNIPAM chains to the anhydride backbone, its grafting density, and the number of the PNIPAM chains on the QD surface. Unfortunately we are unable to separate each of these factors. For our system, it is notoriously difficult to estimate the number of polymer chains in the polymeric

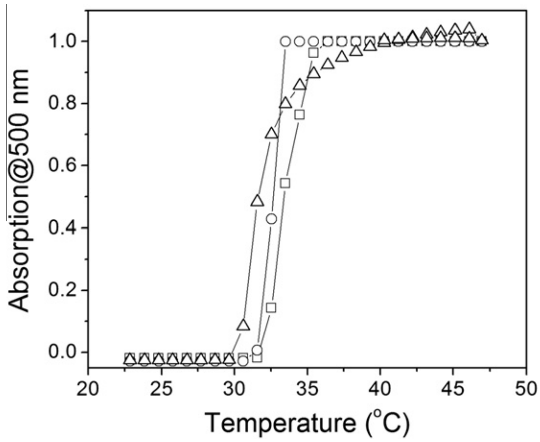

Fig. 3. Normalized absorption of aqueous solutions of amphiphilic polymers **P1** (□), **P10** (○), and **P25** (Δ) measured at 500 nm as a function of temperature.

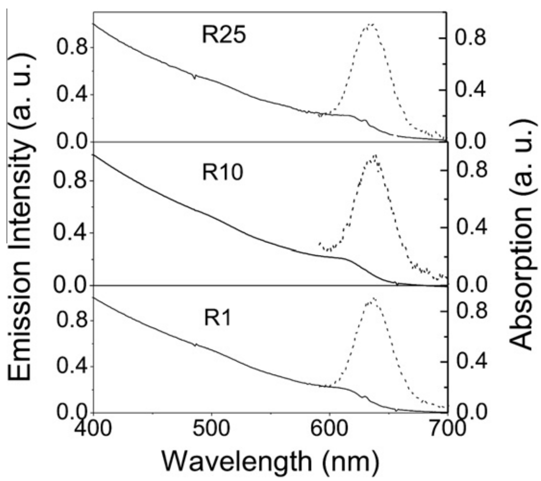

Fig. 4. Normalized emission (dash) and absorption (solid) spectra of water solutions of CdSe/ZnS QDs **R1**, **R10**, and **R25** coated with polymers **P1**, **P10**, and **P25**, respectively.

coating on the QD surface. Additionally, we do not rule out that larger assemblies are formed in water, especially for coatings with longer PNIPAM chains.

Changes in the morphology of the samples upon crossing the LCST of PNIPAM were followed by temperature-dependent light scattering experiments (Fig. 7). Dynamic light scattering (DLS) is a powerful tool to characterize the effective Stokes hydrodynamic size of micro- or nanoparticles, including polymers in solution, and the electrophoretic mobility of charged particles [37]. In principle, if absorbing (and/or luminescent) particles are present in the scattering volume, a complex refractive index must be used in the Rayleigh formalism of light scattering. Chromophore absorption causes intensity loss, heating, and convection effects in the scattering volume. The (incoherent, scattering angle independent) emission intensity is added to the scattered intensity measured. As a result, the scattering function becomes distorted. However, in DLS essentially only local heating can perturb the experiment in routine characterization studies, which can be reduced by low concentration of the particles, low incident light intensity (at the cost of experimental sensitivity), and using a heat dissipating experimental geometry [38]. If proper precautions are taken, DLS can be used with success to characterize the hydrodynamic dimensions, electrophoretic mobility, and stability of water soluble QDs capped with various surface ligands as shown by Mattoussi et al. [39]. In our work we used a low intensity laser and a standard Malvern particle sizer to characterize the QD-PNIPAM assemblies. The error of size measurements ranged from 10% to 15%.

Upon heating to 50 °C, the hydrodynamic radius decreased. A transition was clearly observed at temperatures slightly higher than the onset temperatures of the transitions observed in absorption and luminescence experiments, however, still within the transitions widths.

Temperature dependent electrophoretic mobility experiments shown in Fig. 8 revealed that regardless of the polymeric coating used, the samples displayed low electrophoretic mobility at T < LCST. The particle mobility

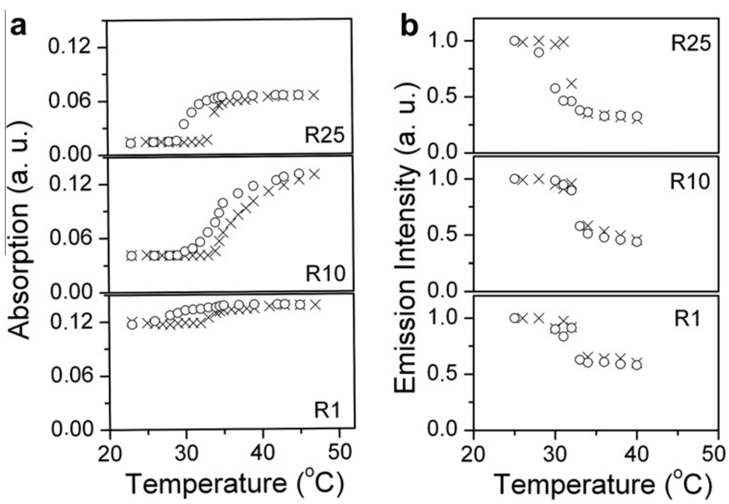

Fig. 5. Absorption at 500 nm (a), and luminescence emission at 640 nm (b) recorded during a heating (X) and subsequent cooling (○) cycle. For comparison, the initial measurements were normalized to 1.0 on the emission plots.

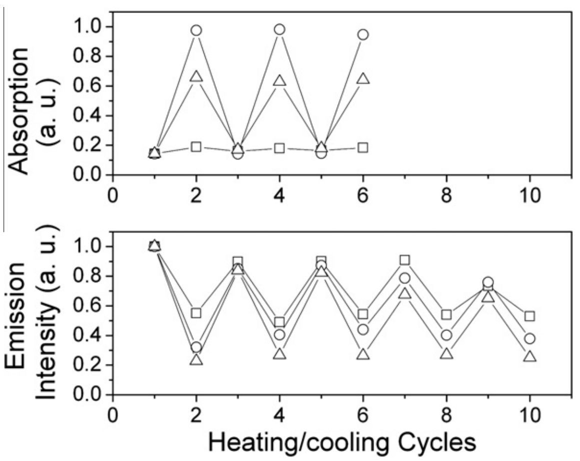

Fig. 6. Optical absorption at 500 nm and emission intensity at λ = 640 nm of **R1** (□), **R10** (○), and **R25** (△) recorded at 25 °C (odd numbers) and at 50 °C (even numbers) in water.

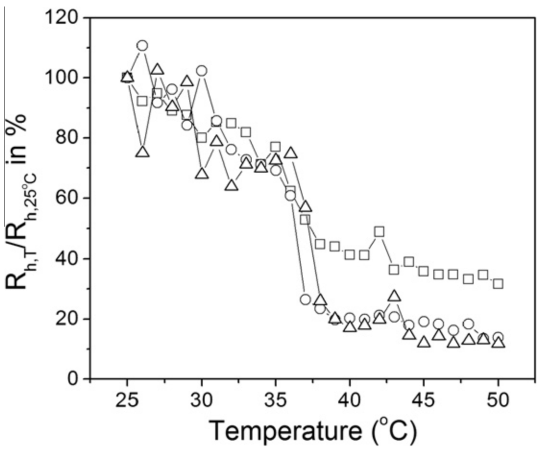

Fig. 7. Effective hydrodynamic radius ($R_{h,T}$) of PNIPAM-coated QDs **R1** (□), **R10** (○), and **R25** (△) as a function of temperature normalized to the hydrodynamic radius at 25 °C ($R_{h,25\,°C}$).

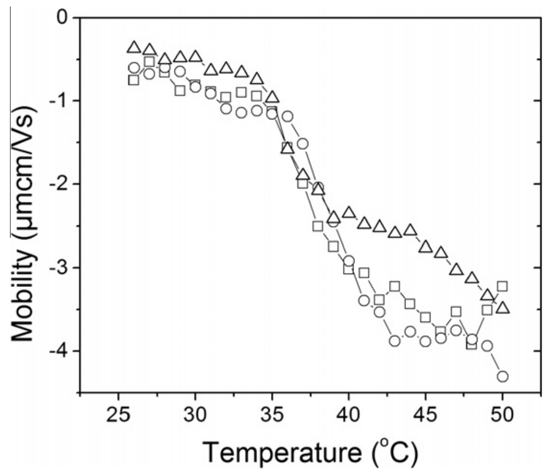

Fig. 8. Electrophoretic mobility of samples **R1** (□), **R10** (○), and **R25** (△) measured as a function of temperature.

was observed to increase sharply as the temperature was raised above the LCST, with a transition onset at temperatures similar to those observed in light scattering experiments. The high electrophoretic mobility above LCST was attributed to the presence of appreciable amount of carboxylic groups on the QD surface. Similar results were obtained by Liu et al. for PNIPAM-coated silica particles [23]. They explained their results by shifts of the shear plane away and closer to the particle surface depending on the morphology of the PNIPAM chains. Exposure of highly hydrophilic carboxylate groups prevents the QDs forming large aggregates [40], what is consistent with the observed decrease of the size of the assemblies upon heating. This is in contrast with previous studies of the LCST behavior of nanoparticles coated with thermoresponsive polymers where the collapse of the polymer chains on the surface of the nanoparticles leads to aggregation [4,28–30].

The above-presented results suggest a complicated process during the LCST transition involving PNIPAM chain collapse and modification of inter-dot interactions resulting in a decrease of the assemblies' size. More studies on the morphology of the samples, which is beyond the scope of this report, are needed to elucidate the exact mechanism for the changes in the luminescence intensity. Regardless, it is important to note that our approach offered an easy QD functionalization protocol based on amphiphilic polymeric coatings, and that the PNIPAM-coated QDs display temperature induced changes in the emission. Additionally the presence of the carboxylate groups on the surface of the QD/polymer assembly prevented aggregation of the QDs below LCST.

4. Conclusions

An efficient method for the fabrication of water soluble, temperature-responsive QD/PNIPAM assemblies was presented. A maleic anhydride-based polymer was used as backbone for grafting PNIPAM chains of three different molar masses. The QDs coated with the polymers were successfully transferred to water. The hybrid nanoparticles exhibited LCST behavior at temperatures similar to those of free polymers. The observed transitions in absorption and luminescence associated with the LCST of PNIPAM were reversible.

Acknowledgement

This project was financially supported by the MESA+ Institute for Nanotechnology, Enschede, The Netherlands.

Appendix A. Supplementary data

Supplementary data associated with this article can be found, in the online version, at doi:10.1016/j.eurpolymj.2010.04.026.

References

[1] Zhang JL, Srivastava RS, Misra RDK. Core–shell magnetite nanoparticles surface encapsulated with smart stimuli-responsive

polymer: synthesis, characterization, and LCST of viable drug-targeting delivery system. Langmuir 2007;23:6342–51.
[2] Hoffman AS, Stayton PS. Conjugates of stimuli-responsive polymers and proteins. Prog Polym Sci 2007;32:922–32.
[3] Narain R, Gonzales M, Hoffman AS, Stayton PS, Krishnan KM. Synthesis of monodisperse biotinylated p(NIPAAm)-coated iron oxide magnetic nanoparticles and their bioconjugation to streptavidin. Langmuir 2007;23:6299–304.
[4] Lai JJ, Hoffman JM, Ebara M, Hoffman AS, Estournes C, Wattiaux A, et al. Dual magnetic-/temperature-responsive nanoparticles for microfluidic separations and assays. Langmuir 2007;23:7385–91.
[5] Tagit O, Tomczak N, Benetti EM, Cesa Y, Blum C, Subramaniam V, et al. Temperature-modulated quenching of quantum dots covalently coupled to chain ends of poly(*N*-isopropyl acrylamide) brushes on gold. Nanotechnology 2009;20:185501–7.
[6] Wang S, Song H, Ong WY, Han MY, Huang D. Positively charged and pH self-buffering quantum dots for efficient cellular uptake by charge mediation and monitoring cell membrane permeability. Nanotechnology 2009;20:425102–10.
[7] Ionov L, Sapra S, Synytska A, Rogach AL, Stamm M, Diez S. Fast and spatially resolved environmental probing using stimuli-responsive polymer layers and fluorescent nanocrystals. Adv Mater 2006;18:1453–7.
[8] Schild HG. Poly(*N*-isopropylacrylamide): experiment, theory and application. Prog Polym Sci 1992;17:163–249.
[9] Schmaljohann D. Thermo- and pH-responsive polymers in drug delivery. Adv Drug Deliv Rev 2006;58:1655–70.
[10] Wu K, Shi L, Zhang W, An Y, Zhu XX. Adjustable temperature sensor with double thermoresponsiveness based on the aggregation property of binary diblock copolymers. J Appl Polym Sci 2006;102:3144–8.
[11] Deng YH, Yang WL, Wang CC, Fu SK. A novel approach for preparation of thermoresponsive polymer magnetic microspheres with core–shell structure. Adv Mater 2003;15:1729–32.
[12] Zhang S, Zhang L, He B, Wu Z. Preparation and characterization of thermosensitive PNIPAA-coated iron oxide nanoparticles. Nanotechnology 2008;19:325608–12.
[13] He J, Chen J-Y, Wang P, Wang P-N, Guo J, Yang W-L, et al. Poly(*N*-isopropylacrylamide)-coated thermo-responsive nanoparticles for controlled delivery of sulfonated Zn-phthalocyanine in Chinese hamster ovary cells in vitro and zebra fish in vivo. Nanotechnology 2007;18:415101–6.
[14] Cheng Z, Liu S, Gao H, Tremel W, Ding N, Liu R, et al. A facile approach for transferring hydrophobic magnetic nanoparticles into water-soluble particles. Macromol Chem Phys 2008;209:1145–51.
[15] Zhu MQ, Wang LQ, Exarhos GJ, Li AD. Thermosensitive gold nanoparticles. J Am Chem Soc 2004;126:2656–7.
[16] Raula J, Shan J, Nuopponen M, Niskanen A, Jiang H, Kauppinen EI, et al. Synthesis of gold nanoparticles grafted with a thermoresponsive polymer by surface-induced reversible-addition-fragmentation chain-transfer polymerization. Langmuir 2003;19:3499–504.
[17] Shan J, Nuopponen M, Jiang H, Kauppinen E, Tenhu E. Amphiphilic gold nanoparticles grafted with poly(*N*-isopropylacrylamide) and polystyrene. Macromolecules 2003;36:4526–33.
[18] Li D, He Q, Cui Y, Wang K, Zhang X, Li J. Thermosensitive copolymer networks modify gold nanoparticles for nanocomposite entrapment. Chemistry 2007;13:2224–9.
[19] Shan J, Nuopponen M, Jiang H, Viitala T, Kauppinen E, Kontturi K, et al. Amphiphilic gold nanoparticles grafted with poly(*N*-isopropylacrylamide) and polystyrene. Macromolecules 2005;38:2918–26.
[20] Shan J, Zhao Y, Granqvist N, Tenhu H. Thermoresponsive properties of *N*-isopropylacrylamide oligomer brushes grafted to gold nanoparticles: effects of molar mass and gold core size. Macromolecules 2009;42:2696–701.
[21] Salmaso S, Caliceti P, Amendola V, Meneghetti M, Magnusson JP, Pasparakis G, et al. Cell up-take control of gold nanoparticles functionalized with a thermoresponsive polymer. J Mater Chem 2009;19:1608–15.
[22] Kim DJ, Kang SM, Kong B, Kim W-J, Paik H-J, Choi H, et al. Formation of thermoresponsive gold nanoparticle/PNIPAAm hybrids by surface-initiated, atom transfer radical polymerization in aqueous media. Macromol Chem Phys 2005;206:1941–6.
[23] Liu J, Pelton R, Hrymak AN. Properties of poly(*N*-isopropylacrylamide)-grafted colloidal silica. J Colloid Interface Sci 2000;227:408–11.
[24] Li D, Jones GL, Dunlap JR, Hua F, Zhao B. Thermosensitive hairy hybrid nanoparticles synthesized by surface-initiated atom transfer radical polymerization. Langmuir 2006;22:3344–51.
[25] Karg M, Pastoriza-Santos I, Liz-Marzan LM, Hellweg T. A versatile approach for the preparation of thermosensitive PNIPAM core–shell microgels with nanoparticle cores. Chem Phys Chem 2006;7:2298–301.
[26] Bruchez Jr M, Moronne M, Gin P, Weiss S, Alivisatos AP. Semiconductor nanocrystals as fluorescent biological labels. Science 1998;281:2013–6.
[27] (a) Tomczak N, Jańczewski D, Han M-Y, Vancso GJ. Designer polymer-quantum dot architectures. Prog Polym Sci 2009;34:393–430;
(b) Jańczewski D, Tomczak N, Han M-Y, Vancso GJ. Stimulus responsive PNIPAM/QD hybrid microspheres by copolymerization with surface engineered QDs. Macromolecules 2009;42:1801–4.
[28] Hou Y, Ye J, Gui Z, Zhang G. Temperature-modulated photoluminescence of quantum dots. Langmuir 2008;24:9682–5.
[29] Ye J, Hou Y, Zhang G, Wu C. Temperature-induced aggregation of poly(*N*-isopropylacrylamide)-stabilized CdS quantum dots in water. Langmuir 2008;24:2727–31.
[30] Zhou L, Gao C, Xu W. Amphibious polymer-functionalized CdTe quantum dots: synthesis, thermo-responsive self-assembly, and photoluminescent properties. J Mater Chem 2009;19:5655–64.
[31] Shiraishi Y, Adachi K, Tanaka S, Hirai T. Effects of poly-*N*-isopropylacrylamide on fluorescence properties of $CdS/Cd(OH)_2$ nanoparticles in water. J Photochem Photobiol A Chem 2009;205:51–6.
[32] Cheng Z, Liu S, Beines PW, Ding N, Jakubowicz P, Knoll W. Rapid and highly efficient preparation of water-soluble luminescent quantum dots via encapsulation by thermo- and redox-responsive hydrogels. Chem Mater 2008;20:7215–9.
[33] Yu WW, Chang E, Falkner JC, Zhang J, Al-Somali AM, Sayes CM, et al. Forming biocompatible and nonaggregated nanocrystals in water using amphiphilic polymers. J Am Chem Soc 2007;129: 2871–9.
[34] Pellegrino T, Manna L, Kudera S, Liedl T, Koktysh D, Rogach AL, et al. Hydrophobic nanocrystals coated with an amphiphilic polymer shell: a general route to water soluble nanocrystals. Nano Lett 2004;4:703–7.
[35] (a) Jańczewski D, Tomczak N, Khin YW, Han MY, Vancso GJ. Designer multi-functional comb-polymers for surface engineering of quantum dots on the nanoscale. Eur Poly J 2009;45:3–9;
(b) Jańczewski D, Tomczak N, Han MY, Vancso GJ. Introduction of quantum dots into PNIPAM microspheres by precipitation polymerization above LCST. Eur Poly J 2009;45:1912–7.
[36] Yu WW, Qu L, Guo W, Peng X. Experimental determination of the extinction coefficient of CdTe, CdSe, and CdS nanocrystals. Chem Mater 2003;15:2854–60.
[37] Berne BJ, Pecora R. Dynamic light scattering with applications to chemistry, biology and physics. New York: Wiley; 1976.
[38] Van Blaaderen A, Vrij A. Synthesis and characterization of colloidal dispersions of fluorescent, monodisperse silica spheres. Langmuir 1992;8:2921–31.
[39] Pons T, Uyeda HT, Medintz IL, Mattoussi H. Hydrodynamic dimensions, electrophoretic mobility, and stability of hydrophilic quantum dots. J Phys Chem B 2006;110:20308–16.
[40] Hou Y, Ye J, Wei X, Zhang G. Effects of cations on the sorting of oppositely charged microgels. J Phys Chem B 2009;113:7457–61.